

The formation of reverted austenite in 18% Ni 350 grade maraging steel

M. FAROOQUE, H. AYUB, A. UL HAQ, A. Q. KHAN

Metallurgy Division, Dr A. Q. Khan Research Laboratories Kahuta, P.O. Box 502, Rawalpindi, Pakistan

E-mail: anwar@isb.comsats.net.pk

Austenite reversion was studied in 18% Ni 350 grade maraging steel. The samples were heat treated from room temperature to the austenite phase field and, without holding, they were cooled again to ambient temperature. The reverted austenite which was retained after this heat treatment was examined using a scanning transmission electron microscope equipped with an energy dispersive spectroscopic system. Two morphologies of the austenite were observed. The first forms at the martensite lath boundaries and the other nucleates inside the martensite laths in the form of Widmanstätten plates. These Widmanstätten plates mostly appear as coupled twins. The coupled twins have a distinct midrib which was found parallel to $(111)_\gamma$ and $(110)_\alpha$ planes. The latter morphology of austenite appeared only after the formation of Ni_3Ti precipitates. Growth of Fe_2Mo precipitates was not observed in this heat-treatment cycle. Both Nishiyama–Wassermann and Kurdjumov–Sachs orientation relationships were found between the austenite and martensite phases. On the basis of these results, it can be suggested that intra-lath-reverted austenite is formed on or by the local dissolution of Ni_3Ti precipitates. © 1998 Kluwer Academic Publishers

1. Introduction

Maraging steels find their application where high toughness, hardness and good magnetic properties are required. Austenite reversion plays a significant role in the magnetic properties of the steel. It has been reported that the remanance, coercive field and the saturation magnetization are related to the austenite content in the martensite matrix [1]. On the other hand, retained austenite deteriorates the mechanical properties of the steel.

Two types of reverted austenite morphologies have been reported in the literature. The first one is the inter-lath austenite which nucleates at the martensite lath boundaries. The other type of austenite is termed the intra-lath reverted austenite, which grows inside the martensite laths in the form of twins. Widmanstätten austenite with a coupled morphology has been reported to be formed in several alloys, e.g. Cu–Zn [2], Fe–Ni–Mn [3] and Fe–Ni–Cr [4] alloys. Viswanathan *et al.* [5] have also observed Widmanstätten austenite in 18% Ni 350 grade maraging steel.

The formation mechanism of these twins is not clear. In the present study an attempt has been made to investigate the nucleation mechanism of reverted austenite, especially of the coupled twin morphology.

2. Experimental procedure

The chemical composition of the 18% Ni 350 grade maraging steel is given in Table I. For heat treatment,

samples of 4 mm × 5 mm × 30 mm size were cut from the annealed material and were encapsulated individually in quartz tubes under a vacuum of 10^{-5} mbar. Heat treatment was carried out using two different heating rates, i.e. 250 and 1000 °C min⁻¹. After heat treatment, thin slices, 0.15 mm thick, were cut using a diamond saw and 3 mm diameter discs were prepared using a spark erosion machine. For electron microscopy, thin foils were prepared by means of a twin-jet electropolisher using a solution of 10% perchloric acid in ethanol. The microstructural and crystallographic investigations were carried out using a scanning transmission electron microscope (STEM) equipped with an energy dispersive spectrometer working at an operating voltage of 200 keV.

3. Results and discussion

Heating rate plays a significant role in the austenite reversion mechanism. Heat treating the martensite matrix at a heating rate of 250 °C min⁻¹ from room temperature to the austenite phase field and cooling again to ambient temperature resulted in the formation of reverted austenite having two types of morphology. The first one, which is the inter-lath reverted austenite grows along the martensite lath boundaries, and the other, which is termed the intra-lath reverted austenite, grows inside the martensite laths in the form of Widmanstätten plates as coupled twins (Fig. 1a). The Widmanstätten plates are acicular in shape and

TABLE I Chemical composition of 18% Ni 350 Grade Maraging Steel (wt %)

Ni	Co	Mo	Ti	Al	C	S	Fe
18	12	4.3	1.7	0.2	0.015	0.003	Bal.

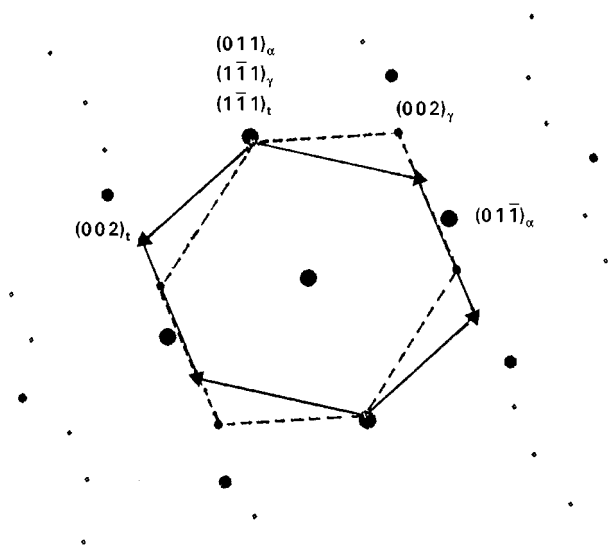
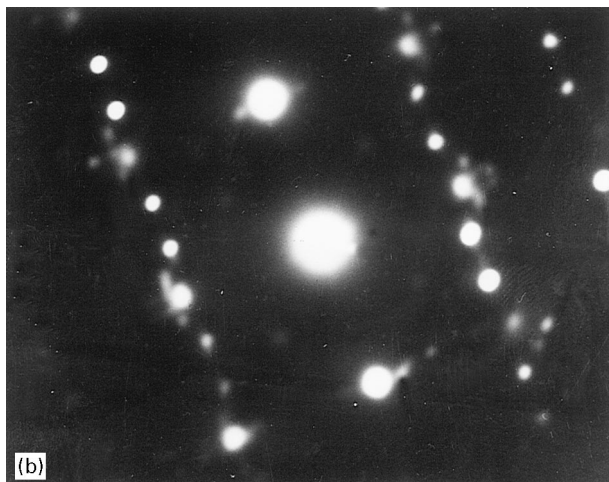
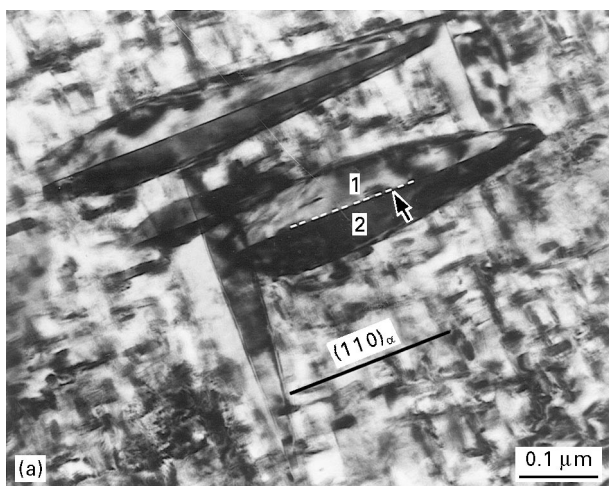


Figure 1 (a) Bright-field TEM image of reverted austenite, (b) the corresponding electron diffraction pattern, and (c) indexed pattern; $Z = [01\bar{1}]_{\alpha}$. The large circles denote α -matrix, the small circles denote γ -spots and the triangles refer to the γ -twin spots.

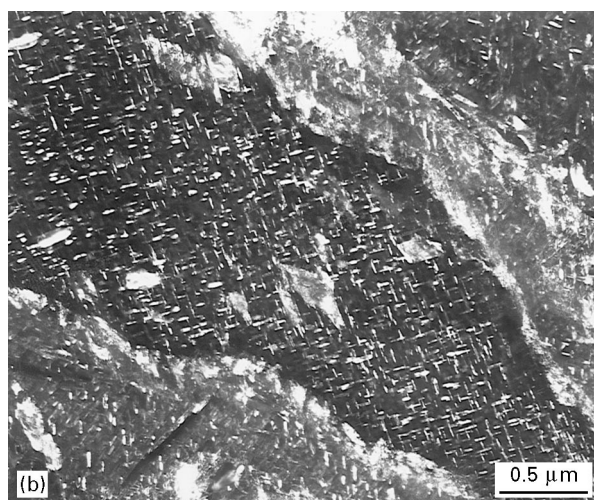
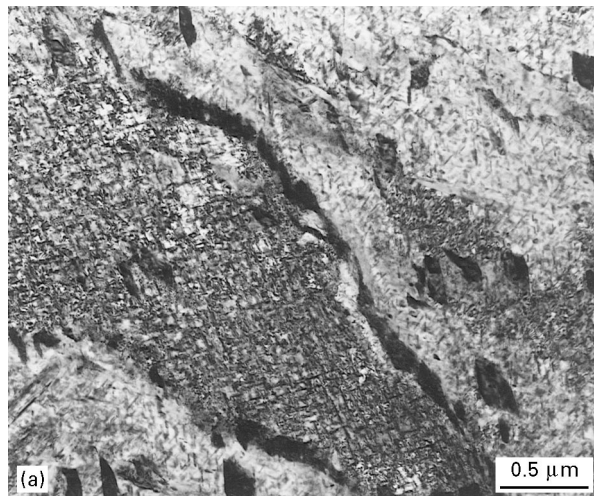


Figure 2 (a) Bright-field TEM image showing the inter-lath reverted austenite grown along the martensite lath boundaries, and (b) the corresponding dark-field image.

have a sharp boundary line in the middle (i.e. midrib) as indicated by the arrows. Fig. 1b and c represent the corresponding electron diffraction pattern and the indexed pattern, respectively. It can be easily seen that austenite along both sides of the midrib is twin related and the midrib is parallel to the $(111)_{\gamma}$ and $(110)_{\alpha}$ planes. These coupled plates were each found to obey the Nishyama–Wassermann [6] orientation relationship with the matrix, as given below

$$\begin{aligned} \{100\}_{\alpha} \parallel \{110\}_{\gamma} \\ \{011\}_{\alpha} \parallel \{1\bar{1}1\}_{\gamma} \end{aligned}$$

Inter-lath reverted austenite is nucleated on the martensite lath boundaries. The image and corresponding electron diffraction pattern are presented in Fig. 2a and b, respectively. A Kurdjumov–Sachs [7] orientation relationship has also been found between both the inter-lath and the intra-lath austenites and the martensite phase. However, there is a difference of only 6° between the Nishyama–Wassermann and Kurdjumov–Sachs orientation relationships.

In addition to the above mentioned phases, Ni_3Ti precipitates are seen finely distributed throughout the martensite matrix which is presented in the

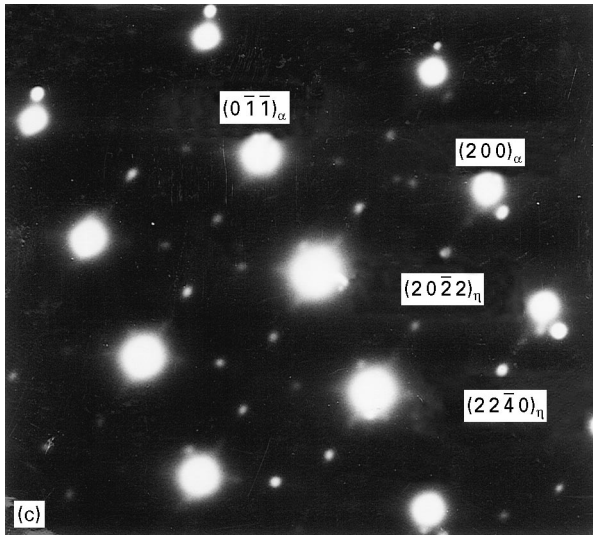
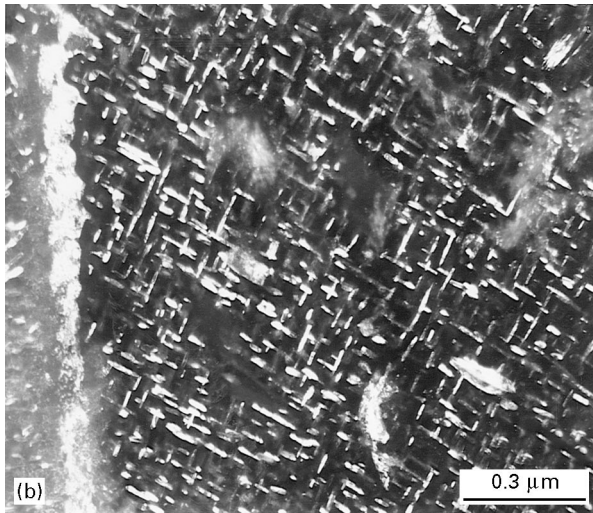
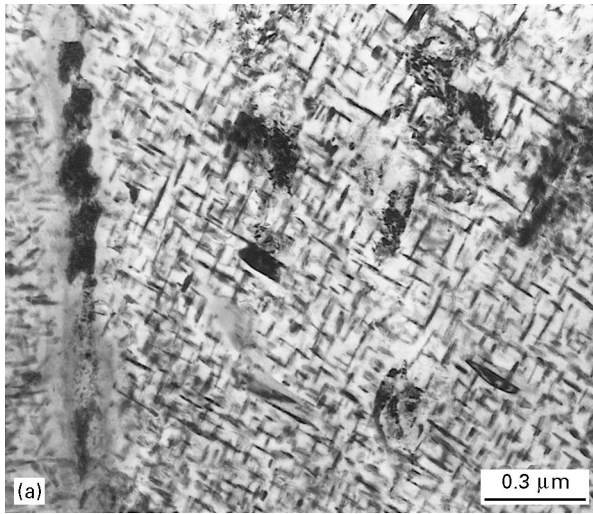


Figure 3 (a) Bright-field transmission electron micrograph showing the growth of Ni_3Ti precipitates inside the martensite matrix, (b) the corresponding dark-field image with the precipitates highlighted, and (c) the corresponding electron diffraction pattern with the indexed planes marked.

bright-field micrograph in Fig. 3a. The corresponding diffraction pattern (Fig. 3c) shows reflections of both precipitates and martensite matrix. The measured interplanar spacings of the different precipitate spots are

TABLE II EDS analysis

Elements (wt %)	Inter-lath austenite	Intra-lath austenite
Fe	59	57
Ni	21.6	24
Co	10	9.8
Mo	6.9	7
Ti	1.7	1.8

in accordance with the $\eta\text{-Ni}_3\text{Ti}$ phase. The observed orientation relationship, as reported by Vasudevan *et al.* [8] between martensite and $\eta\text{-Ni}_3\text{Ti}$ is

$$\{01\bar{1}\}_\alpha \parallel \{0001\}_\eta$$

$$\langle 111 \rangle_\alpha \parallel \langle 11\bar{2}0 \rangle_\eta$$

Heat treatment carried out at a faster heating rate of $1000^\circ\text{C min}^{-1}$ does not result in the nucleation of γ -twins, although inter-lath reverted austenite is observed grown on the martensite lath boundaries.

Nickel and molybdenum are both austenite stabilizers. It has been suggested by Sha *et al.* [9] that Ni_3Ti precipitates are molybdenum enriched and they are formed in the early stages of ageing and molybdenum cosegregates with nickel in Ni_3Ti precipitates. Another type of precipitate is the Fe_2Mo which is mostly formed at overageing temperatures. It is observed that whenever Fe_2Mo precipitates are formed, coupled morphology of the austenite is not observed in the specimen. This is because most of the molybdenum is consumed in the precipitation of Fe_2Mo precipitates and the rest of the molybdenum present in the matrix is partly consumed by the inter-lath γ -nucleation on the martensite lath boundaries.

It has been suggested by Goldberg [10], that Ni_3Ti precipitates, which are mostly observed to grow inside the martensite matrix, serve as the nucleation sites for the intra-lath reverted austenite formation.

This is further confirmed by an analysis carried out on the scanning transmission electron microscope between the inter-lath and the intra-lath reverted austenite. Table II shows the difference in chemical composition of the two austenites. It is evident that the intra-lath reverted austenite is rich in nickel and molybdenum content, which suggests that a depleted region and an enriched region is obtained because of segregation of the alloying elements. This means that the intra-lath austenite is grown on the Ni_3Ti precipitate sites, which are basically the enriched regions, having higher contents of nickel and molybdenum, and are formed by the dissolution of these precipitates, which leads to local nickel enrichment [11]. Nickel and molybdenum actually stabilize the austenite at room temperature [10], as they are present in higher concentration.

Microstructural observations and EDS analysis suggest that the intra-lath reverted austenite is formed by the dissolution of Ni_3Ti precipitates. Another support for this hypothesis is given by Yu. Frolova *et al.* [12]. They experimented on the alloy Fe-27 wt %

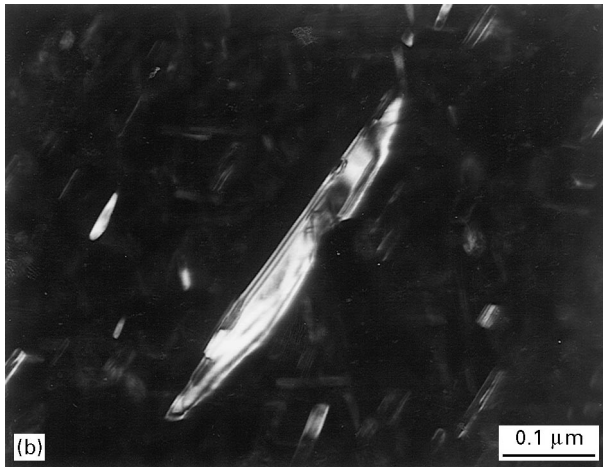
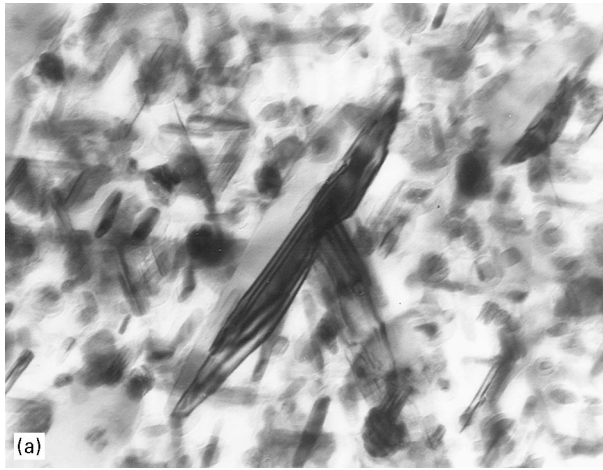


Figure 4 (a) Bright-field TEM image showing a large and a small twin grown inside the martensite matrix, and (b) the corresponding dark-field image.

Ni-2 wt % Ti. Ageing the alloy resulted in the formation of only the Ni_3Ti phase. On further heating, electron microscopic examination revealed numerous austenite crystals inside the martensite phase.

The morphology, orientation relationship and mid-rib of the intra-lath reverted austenite suggest that it nucleates by a diffusionless transformation mechanism and grows further by a diffusion-controlled shear motion [13].

Twinned morphology of reverted austenite, which is obtained by heating in the austenite phase field, suggests that the steel initially passes through the precipitation region and as a result Ni_3Ti precipitates are formed. As the alloy reaches the A_s (austenite start) temperature, frequent austenite grains are formed inside the martensite matrix in the form of twins. Nucleation sites of these twins are preferably the

nickel-enriched regions which are formed by the dissolution of Ni_3Ti particles.

The bright-field and the corresponding dark-field images presented in Fig. 4a and b show a small and a large twin. This suggests that a large precipitate nucleates as a twin even at a very early stage.

4. Conclusions

1. At a heating rate of $250^\circ\text{C min}^{-1}$, Ni_3Ti precipitates, inter-lath and intra-lath reverted austenites are formed. The reverted austenite has Nishyama-Wassermann and Kurdjumov-Sachs orientation relationships with the martensite matrix.

2. The faster heating rate of $1000^\circ\text{C min}^{-1}$ eliminated the formation of Ni_3Ti precipitates and hence the coupled twin morphology of Widmanstätten austenite is not observed, which confirms that these plates nucleate on Ni_3Ti precipitates.

3. It is suggested that the nucleation of γ -twins is a diffusionless transformation mechanism and they further grow by a diffusion-controlled shear transformation mechanism.

Acknowledgement

The authors thank Mr Afzal Hussain for metallography and photographic work.

References

1. M. AHMED, A. ALI, S. K. HASNAIN, F. H. HASHMI and A. Q. KHAN, *Acta Metall. Mater.* **42** (1994) 631.
2. J. PERKINS, *Metallography* **6** (1973) 185.
3. G. THOMAS, I-LIN CHENG and J. R. MIHALISM, *Trans. ASM* **9** (1969) 421.
4. T. ARAKI, H. MAUSI and K. SHIBATA, *Trans. JIM* **9** (1968) 421.
5. U. K. VISWANATHAN, G. K. DEY and M. K. ASUNDI, *Metall. Trans.* **24A** (1993) 2429.
6. Z. NISHIYAMA, *Sci. Rep. Tohoku Univ.* **23** (1934) 638.
7. G. KUDJUMOV and G. SACHS, *Z. Phys.* **64** (1930) 325.
8. VIJAY K. VASUDEVAN, SUNG J. KIM and C. M. WAYMAN, *Metall. Trans.* **21A** (1990) 2655.
9. W. SHA, A. CEREZO and G. D. W. SMITH, *ibid.* **24A** (1993) 1251.
10. A. GOLDBERG, *Trans. ASM* **61** (1968).
11. V. I. ZELDOVICH and N. YU. FROLOVA, *Fiz. Metal. Metalloved.* **2** (1990) 175.
12. N. YU. FROLOVA, V. I. ZELDOVICH and YU. I. FILIPPOV, *ibid.* **7** (1991) 153.
13. L. T. SHIANG and C. M. WAYMAN, *Metallography* **21** (1988) 425.

Received 4 October 1996
and accepted 3 March 1998